

Analysis of a map-based neuronal model

G. Moza*, R. Efrem†

Abstract

Subthreshold oscillations in neurons are those oscillations which do not attain the critical value of the membrane's voltage needed for triggering an action potential (a spike). Their contribution to the forming of action potentials in neurons is a current field of research in biology. The present work approaches this subject using tools from mathematical modeling, more exactly, a neuronal non-smooth map-based model is proposed and studied. The behavior of the model in a noisy medium is also studied.

1 Introduction

Neuronal activity is a continuous challenge both for common people and researchers. One of the pioneering works from this domain is [10], where the authors describe how action potentials (electrical impulses, spikes) are formed in the central part of a neuron. A bio-mathematical model based on four differential equations has been proposed and studied in this work to explain the process of forming action potentials. More other models have been proposed since then in an effort to better understand how neurons work. The research field is of current interest and new models based on differential equations or difference equations (map-based) are proposed. Neuronal map-based models have been studied lately, for example, in [1]–[7], [15], [17], [22], [23] and in some references therein.

While many models study various patterns of action potentials, in [18] is proposed a model that focuses on precursory oscillations to spiking activity. Experimental data suggest that some neurons are brought out from the silence regime not abruptly but slowly through small oscillations [12]. These oscillations below the subthreshold of observable spikes may shape the spiking neuronal activity when the membrane gets depolarized or hyperpolarized [13]. Two discrete-time phenomenological models trying to explain how subthreshold oscillations shape spiking-bursting neuron oscillations are proposed in [18] and [19]. The models are in the form of a two-dimensional non-smooth map (discrete-time system) given by

$$\begin{aligned} X_{n+1} &= f_a(X_n, Y_n) \\ Y_{n+1} &= Y_n - m(X_n + 1 - s) \end{aligned} \quad (1)$$

$n \geq 0$, where $f_a : \mathbb{R}^2 \rightarrow \mathbb{R}$ is a piecewise differentiable function with $m \geq 0$ and $s \in \mathbb{R}$. The system is of non-smooth type because f_a is a non-smooth function. The X -variable in (1) describes the dynamics of the neuron's transmembrane potential while the parameters a, m, s control individual dynamics of the system [16]. A recent study on two Rulkov models of type (1) has been reported in [6]. The map studied in [18] is able to generate stable subthreshold oscillations while the map proposed in [19] unstable subthreshold oscillations. In [16] $f_a(x, y)$ is of the form $f_a(x, y + \beta)$ to provide links with other models. In this work we aim to introduce

*Department of Mathematics, Politehnica University of Timisoara, P-ta Victoriei, Nr.2, 300006, Timisoara, Timis, Romania; email: gheorghe.moza@upt.ro

†Department of Mathematics, University of Craiova, Romania

a new model by changing the expression of the function f_a in (1). More exactly, we propose an *exponential branch* in the definition of f_a instead of a *parabola* or *hyperbola* used in the above-mentioned models [18], [19].

The paper is organized as follows. After an introductory section, in Section 2 we define our neuronal map-based two-dimensional model and point out the first properties of it. In Sections 3 and 4 we proceed to the bifurcation analysis of the main part of the model. In Section 5 we investigate the map subjected to noises. Numerical studies show that the map captures the phenomenon of vulnerability to noise of action potentials. More exactly, subthreshold activity of the map in a noisy medium gives rise to spikes. Moreover, we observed that our map in the presence of noise is brought out to a spiking activity directly from the silence regime. Conclusions are presented in the last section of the paper.

2 Defining the model. Bifurcations

In the present work we consider the system (1) with a function $f_a : \mathbb{R}^2 \rightarrow \mathbb{R}$ given by

$$f_a(x, y) = \begin{cases} -a^2 - e^{-a} + y, & \text{if } (x, y) \in D_1 \\ ax - e^x + y, & \text{if } (x, y) \in D_2 \\ a(y+1) - e^{y+1} + y, & \text{if } (x, y) \in D_3 \\ -1, & \text{if } (x, y) \in D_4 \end{cases} \quad (2)$$

where

$$D_1 = \{(x, y) \in \mathbb{R}^2 : x < -a\}, D_2 = \{(x, y) \in \mathbb{R}^2 : x \geq -a, x < y + 1\}, \\ D_3 = \{(x, y) \in \mathbb{R}^2 : x \geq -a, y + 1 \leq x < y + 2\} \text{ and } D_4 = \{(x, y) \in \mathbb{R}^2 : x \geq -a, x \geq y + 2\}.$$

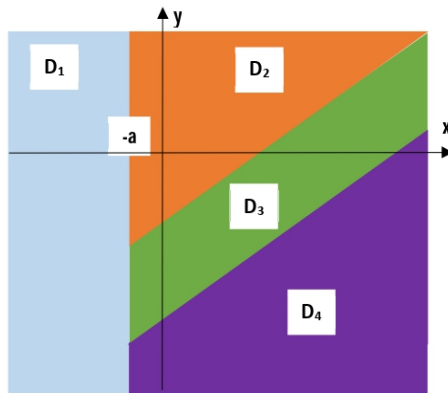


Figure 1: The four planar sets $D_1 - D_4$ forming the domain of definition of the function f_a for $a > 0$.

When referring further in this work at the system (1) we consider that f_a is given by (2). The function f_a is piecewise smooth. It is continuous on the borders D_{12} and D_{23} and discontinuous on D_{13} , D_{14} and D_{34} , where D_{12} denotes the border between the domains D_1 and D_2 , and similarly for the other borders. The domains $D_1 - D_4$ and their borders are sketched in Fig.1. For those values of m small enough, $0 < m \ll 1$, the system (1) is of slow-fast type; the first equation in (1) is termed the fast subsystem while the second the slow subsystem.

Remark 2.1. *The reason we propose an exponential branch in the expression of the function f_a is to see if exponential terms bring new types of oscillations of the map (1), new patterns of oscillations both in the*

subthreshold and spiking activity regimes, or a larger spectrum of stability, compared with the models studied in [18] and [19] which use parabola or hyperbola terms.

The main dynamics of the system (1) is described by the second branch of f_a since it has the both variables x and y . The other branches are some kind of limiters. Hence, we will study in the following the system

$$\begin{aligned} X_{n+1} &= aX_n - e^{X_n} + Y_n \\ Y_{n+1} &= Y_n - m(X_n + 1 - s) \end{aligned} \quad (3)$$

with $-a \leq X_n < Y_n + 1$, and $a, s \in \mathbb{R}$, $m \geq 0$.

We study first (3) at $m = 0$. In this case, the second equation in (3) is independent from the first and $Y_n = Y_0$, for all $n \geq 0$. Hence, Y_0 becomes a real parameter in the first equation. Depending on a and Y_0 , the system can have zero, one or two fixed points. More exactly, if $a < 1$ it has a single fixed point for any fixed real Y_0 , at $a = 1$ it has no fixed points for $Y_0 \leq 0$ and one fixed point $X = \ln Y_0$ for $Y_0 > 0$, while for $a > 1$ it can have zero, one or two fixed points. Let us detail the latter case, $a - 1 > 0$. Denote by

$$h(x) = (a - 1)x - e^x + Y_0$$

and $x_0 = \ln(a - 1)$ the root of $h'(x) = 0$. Notice that $h(\infty) = -\infty$ and $h(-\infty) = -\infty$. Therefore, if $h(x_0) < 0$ the system (3) has no fixed points while if $h(x_0) = 0$, it has a unique fixed point $X = x_0$. When $h(x_0) > 0$, the system has two different fixed points denoted by $X_{1,2}(a, Y_0)$ which satisfy $X_1 < \ln(a - 1) < X_2$. From

$$\frac{\partial X_{n+1}}{\partial X_n} = a - e^{X_n},$$

it follows that X_1 is unstable whenever it exists, that is on $X < \ln(a - 1)$, respectively, X_2 is stable for $\ln(a - 1) < X_2 < \ln(a + 1)$ and unstable for $X_2 > \ln(a + 1)$. For example, if $a = e + 1$ and $Y_0 = 1$, we find $X_1 = 0$ and $X_2 \simeq 1.752$.

Assume further $m > 0$. The system (3) has a unique fixed point $A(s - 1, (1 - a)(s - 1) + e^{s-1})$ in this case, provided that the parameters satisfy the inequality $-a < s - 1 < a + (1 - a)s + e^{s-1}$. Introducing the new coordinates

$$\begin{pmatrix} X \\ Y \end{pmatrix} = \begin{pmatrix} x + s - 1 \\ y + (1 - a)(s - 1) + e^{s-1} \end{pmatrix},$$

the map (3) becomes

$$\begin{aligned} \tilde{x} &= y + ax + e^{s-1} - e^{x+s-1} \\ \tilde{y} &= y - mx \end{aligned} \quad (4)$$

where $a, s \in \mathbb{R}$ and $m > 0$. In (4) and in other discrete systems below we will use the notations $(\tilde{x}, \tilde{y}) = (x_{n+1}, y_{n+1})$ and $(x, y) = (x_n, y_n)$ for all $n \geq 0$. The new map (4) is defined on

$$-a \leq s - 1 + x < a + (1 - a)s + e^{s-1} + y$$

and has a unique fixed point $O(0, 0)$. Its Jacobian at O is $J = \begin{pmatrix} a - e^{s-1} & 1 \\ -m & 1 \end{pmatrix}$ with the eigenvalues (multipliers)

$$\lambda^\pm = \frac{1}{2} \left(a - e^{s-1} + 1 \pm \sqrt{(e^{s-1} - a + 1)^2 - 4m} \right). \quad (5)$$

Since $m > 0$, two main bifurcations may appear in (4), namely period-doubling and Neimark-Sacker.

3 Period-doubling bifurcations

Assume first $(e^{s-1} - a + 1)^2 \geq 4m$, hence λ^\pm are real. Notice that $\lambda^\pm \neq 1$ since $m > 0$, thus, a fold bifurcation is not possible. Denote further by

$$m_0 = 2(e^{s-1} - a - 1)$$

whenever $e^{s-1} - a - 1 > 0$. Then, $\lambda^+ = -1$ and $\lambda^- = a - e^{s-1} + 2$ if $m_0 > 4$ and $m = m_0$, respectively, $\lambda^- = -1$ and $\lambda^+ = a - e^{s-1} + 2$ if $0 < m_0 < 4$ and $m = m_0$. At $m = m_0 = 4$, we have $\lambda^+ = \lambda^- = -1$. Thus, a *period-doubling bifurcation* occurs in the system (4) at $m = m_0$, which is also known as the *flip* bifurcation. In order to study this bifurcation we need to reduce the system (4) to the center manifold through $O(0,0)$. The next theorem from [11] will be useful to our study.

Theorem 3.1. *Assume the one-dimensional discrete system*

$$\tilde{x} = f(x, m), \tag{6}$$

f sufficiently smooth, $x, \tilde{x}, m \in \mathbb{R}$, has at $m = 0$ a fixed non-hyperbolic point $x_0 = 0$ with the multiplier $\mu = f_x(0, 0) = -1$. Consider that the following two nondegeneracy (generic) conditions hold:

$$pd1) c(0) \stackrel{def}{=} \frac{1}{4} \left(\frac{\partial^2 f}{\partial x^2}(0, 0) \right)^2 + \frac{1}{6} \frac{\partial^3 f}{\partial x^3}(0, 0) \neq 0,$$

$$pd2) \frac{\partial^2 f}{\partial x \partial m}(0, 0) \neq 0.$$

Then, the system (6) is locally topologically equivalent near the origin to the following normal form

$$\tilde{\xi} = -(1 + \beta(m))\xi + s\xi^3, \tag{7}$$

where $s = \text{sign}(c(0))$ and $\beta(m) = -1 - \frac{\partial f}{\partial x}(0, m)$.

To this end, consider further the extended form of (4)

$$\begin{aligned} \tilde{m} &= m \\ \tilde{x} &= y + x(a - e^{s-1}) - \frac{1}{2}x^2e^{s-1} - \frac{1}{6}x^3e^{s-1} + O(x^4) \\ \tilde{y} &= y - mx \end{aligned} \tag{8}$$

which has the non-hyperbolic fixed point $(m_0, 0, 0)$ with the multipliers $\lambda_1 = 1$, $\lambda_2 = -1$ and $\lambda_3 = a - e^{s-1} + 2$. Assume further $m_0 \neq 4$, thus, $\lambda_3 \neq \pm 1$. We used the Taylor expansion of e^{x+s-1} at $x = 0$ in (8). Hence, there exists a 2-dimensional center manifold W^c of equation $y = y(m, x)$ and $(m_0, 0, 0) \in W^c$, given locally by:

$$\begin{aligned} W^c : y &= a_1(m - m_0) + a_2(m - m_0)^2 + a_3(m - m_0)^3 + b_1x + b_2x^2 + b_3x^3 \\ &+ c_1(m - m_0)x + c_2(m - m_0)x^2 + c_3(m - m_0)^2x + \dots \end{aligned} \tag{9}$$

Then

$$\begin{aligned} \tilde{y} &= a_1(\tilde{m} - m_0) + a_2(\tilde{m} - m_0)^2 + a_3(\tilde{m} - m_0)^3 + b_1\tilde{x} + b_2\tilde{x}^2 + b_3\tilde{x}^3 \\ &+ c_1(\tilde{m} - m_0)\tilde{x} + c_2(\tilde{m} - m_0)\tilde{x}^2 + c_3(\tilde{m} - m_0)^2\tilde{x} + \dots \end{aligned}$$

Using now (8) and (9), we find that $a_1 = 0, a_2 = 0, a_3 = 0, b_1 = \frac{m_0}{2}, b_2 = \frac{1}{2}e^{s-1}, b_3 = -\frac{1}{6}e^{s-1}\frac{m_0}{4-m_0}, c_1 = \frac{2}{4-m_0}, c_2 = \frac{4e^{s-1}}{m_0(4-m_0)}, c_3 = \frac{8}{(4-m_0)^3}$.

Finally, the system (8) restricted to the central manifold is 1-dimensional and for $|m - m_0|$ small enough it reads

$$\tilde{x} = x\sigma_1 + x^2\sigma_2 + x^3\sigma_3 + O(x^4) \stackrel{not}{=} f(x, m) \quad (10)$$

where $\sigma_1 = \frac{2(4-m_0)^2(m-m_0)+8(m-m_0)^2}{(4-m_0)^3} - 1$, $\sigma_2 = \frac{4e^{s-1}(m-m_0)}{m_0(4-m_0)}$ and $\sigma_3 = -\frac{2e^{s-1}}{3(4-m_0)}$.

Because the hyperplanes $U_m = \{(m, x, y) : m = const\}$ are invariant with respect to the map (8), the manifold W^c is foliated by the 1-dimensional invariant manifolds

$$W_m^c = W^c \cap U_m.$$

This manifold W_m^c is a local invariant parameter-dependent manifold of the initial system (4). Then (10) has the multiplier $\mu = \frac{\partial f}{\partial x}(0, m_0) = -1$ while $\frac{\partial^2 f}{\partial x \partial m}(0, m_0) = \frac{\partial \sigma_1}{\partial m}(m_0) = -\frac{2}{m_0-4} \neq 0$; $m_0 \neq 4$. Further,

$$c(0) = \frac{1}{4} \left(\frac{\partial^2 f}{\partial x^2} \right)^2 + \frac{1}{6} \frac{\partial^3 f}{\partial x^3} = \sigma_2^2 + \sigma_3 = \frac{2e^{s-1}}{3(m_0-4)} \neq 0.$$

Hence pd1)-2) are satisfied. The coefficient $c(0)$ can be obtained also by another method [11]. Indeed, denote by $z = \begin{pmatrix} x \\ y \end{pmatrix}$. Using the Taylor expansion of e^{x+s-1} at $x = 0$, the system (4) when $m = m_0$ can be put in the form

$$\tilde{z} = Jz + \frac{1}{2}B(z, z) + \frac{1}{6}C(z, z, z),$$

where $B(z, u) = \begin{pmatrix} -xx_1e^{s-1} \\ 0 \end{pmatrix}$, $C(z, u, v) = \begin{pmatrix} -xx_1x_2e^{s-1} \\ 0 \end{pmatrix}$ and $u = \begin{pmatrix} x_1 \\ y_1 \end{pmatrix}$, $v = \begin{pmatrix} x_2 \\ y_2 \end{pmatrix}$ are two vectors. An eigenvector for $\lambda^- = -1$ is $q = \begin{pmatrix} 1 \\ e^{s-1} - a - 1 \end{pmatrix}$. An adjoint eigenvector p to q , i.e. $J^T p = -p$, such that $\langle p, q \rangle = 1$, is $p = \begin{pmatrix} \frac{2}{a-e^{s-1}+3} \\ -\frac{1}{a-e^{s-1}+3} \end{pmatrix}$. We can determine now the coefficient $c(0)$ from the formula

$$\begin{aligned} c(0) &= \frac{1}{6} \langle p, C(q, q, q) \rangle - \frac{1}{2} \langle p, B(q, (J - I_2)^{-1} B(q, q)) \rangle \\ &= \frac{1}{6} \langle p, C(q, q, q) \rangle = \frac{4e^{s-1}}{m_0 - 4}. \end{aligned}$$

We notice the expressions of $c(0)$ obtained with the two methods differ by a positive constant but $s = \text{sign}(c(0))$ is the same. In fact $c(0)$ is not unique, it depends on the vectors p and q .

Hence, a period-doubling bifurcation occurs at $m = m_0$ and the system (10) is locally topologically equivalent near the origin to the normal form

$$\tilde{\xi} = -(1 + \beta(m))\xi + s\xi^3, \quad (11)$$

where $s = +1$ if $m_0 > 4$ and $s = -1$ if $0 < m_0 < 4$. Here

$$\beta(m) = -1 - \sigma_1 = 2 \left(4(m - m_0) + (m_0 - 4)^2 \right) \frac{m - m_0}{(m_0 - 4)^3}$$

with $\beta(m_0) = 0$ and $\frac{\partial \beta}{\partial m}(m_0) = \frac{2}{m_0-4} \neq 0$.

This means that a cycle of period two bifurcates at $m = m_0$ in (11). Assume first $s = -1$ and $0 < m_0 < 4$. Denoting by $g(\xi) = -(1 + \beta)\xi - \xi^3$, one can show that $g^2(\xi) = g(g(\xi))$ has two nontrivial fixed points depending on a sufficiently small β with $\beta < 0$ given by

$$\xi_{1,2} = \pm \sqrt{-\beta} + O(\beta),$$

that is, $g_m^2(\xi_{1,2}) = \xi_{1,2}$. These two points form a period-two *unstable* cycle of the map (10), i.e. $\xi_1 = f(\xi_2, m)$ and $\xi_2 = f(\xi_1, m)$. The cycle vanishes for $\beta \geq 0$. The higher-order terms in (10) do not affect the bifurcation. In the second case, $s = +1$ and $m_0 > 4$, $g^2(\xi)$ has two nontrivial fixed points in the form $\xi_{1,2} = \pm\sqrt{\beta} + O(\beta)$ which form a *stable* cycle of the map (10). Concluding, we have the following theorem.

Theorem 3.2. *If $0 < m \leq \frac{(m_0+4)^2}{16}$ the system (4) undergoes a period-doubling bifurcation at m_0 . More exactly, if $0 < m_0 < 4$ (respectively, $m_0 > 4$) a period-two unstable (respectively, stable) cycle is born for $0 < m < m_0 - \frac{1}{4}(m_0 - 4)^2$ or $m > m_0$.*

Remark 3.3. *Of practical interest is the case $0 \leq m \ll 1$ and, because the bifurcation occurs at $m = m_0$, this yields $0 \leq m_0 \ll 1$. Thus, we are in the case with $s = -1$ and $\beta(m) < 0$, which is equivalent to $m > m_0$, since m_0 is sufficiently small. It follows that, the period-doubling bifurcations may occur when the parameters lie in the zones of practical interest and contribute to the formation of action potentials in the model (1). This represents an added value of our model compared to other models (see e.g. [18]) in which period-doubling bifurcations occur outside the zone of practical interest.*

4 Neimark-Sacker bifurcation

In order to study this bifurcation in our map (4), we describe it in a general setup first to ease its presentation (see e.g. [11]). Consider a discrete-time system

$$\tilde{x} = f(x, \alpha), x = (x_1, x_2) \in \mathbb{R}^2, \alpha \in \mathbb{R},$$

f sufficiently smooth, having for all $|\alpha|$ small enough a fixed point $x_0 = (0, 0)$ with the multipliers $\mu_{1,2}(\alpha) = r(\alpha)e^{\pm i\theta(\alpha)}$, where $r(0) = 1$, $\theta(0) = \theta_0$ and $0 < \theta_0 < \pi$. The system can be put in the form

$$\tilde{x} = A(\alpha)x + F(x, \alpha), \quad (12)$$

where $\mu_{1,2}(\alpha)$ are the eigenvalues of the Jacobian matrix $A(\alpha)$. The radius r can also be written in the form $r(\alpha) = 1 + \beta(\alpha)$ for some smooth functions $\beta(\alpha)$ with $\beta(0) = 0$. Assume $\beta'(0) \neq 0$ and consider β as a new parameter of the system. Then the multipliers are of the form $\mu(\beta), \bar{\mu}(\beta)$ where $\mu(\beta) = (1 + \beta)e^{i\theta(\beta)}$, with $\theta(\beta)$ a smooth function such that $\theta(0) = \theta_0$. In complex variables $z = x_1 + ix_2$, $\bar{z} = x_1 - ix_2$, the equation (12) can be put, for $|\beta|$ small enough, in the form

$$\tilde{z} = \mu(\beta)z + g(z, \bar{z}, \beta),$$

where $\beta \in \mathbb{R}$, $z \in \mathbb{C}$, $\mu(\beta) = (1 + \beta)e^{i\theta(\beta)}$, $\mu_0 = e^{i\theta_0}$, and g is a smooth complex function of z, \bar{z}, β whose Taylor expansion in (z, \bar{z}) begins with at least quadratic terms,

$$g(z, \bar{z}, \beta) = \sum_{i+j \geq 2} \frac{1}{i!j!} g_{ij}(\beta) z^i \bar{z}^j.$$

Theorem 4.1. *(Generic Neimark-Sacker bifurcation) Assume the two-dimensional one-parameter system*

$$\tilde{x} = f(x, \alpha) \quad (13)$$

$x \in \mathbb{R}^2$, $\alpha \in \mathbb{R}$, has for all $|\alpha|$ small enough a fixed point $x_0 = (0, 0)$ with the multipliers $\mu_{1,2}(\alpha) = r(\alpha)e^{\pm i\theta(\alpha)}$, where $r(0) = 1$, $\theta(0) = \theta_0$, such that $\frac{dr}{d\alpha}(0) \neq 0$ and $e^{ik\theta_0} \neq 1$ for $k = 1, 2, 3, 4$. Denote by

$$c_1(0) = \frac{g_{20}(0)g_{11}(0)(1 - 2\mu_0)}{2(\mu_0^2 - \mu_0)} + \frac{|g_{11}(0)|^2}{1 - \bar{\mu}_0} + \frac{|g_{02}(0)|^2}{2(\mu_0^2 - \bar{\mu}_0)} + \frac{g_{21}(0)}{2}, \quad (14)$$

where $\mu_0 = e^{i\theta_0}$. Then, the map (13) is locally topologically equivalent near the origin x_0 for all $|\alpha|$ small enough to the map in polar coordinates given by

$$\begin{cases} \tilde{\rho} = \rho(1 + \beta + d(\beta)\rho^2) + \rho^4 R(\beta, \rho) \\ \tilde{\varphi} = \varphi + \theta(\beta) + \rho^2 Q(\beta, \rho) \end{cases} \quad (15)$$

where $\beta(\alpha) = r(\alpha) - 1$ and $d(0) = \text{Re}(e^{-i\theta_0} c_1(0))$.

The first equation in (13), the ρ -map, is independent of φ and can be analyzed separately as a one-dimensional map. It has two fixed points, $\rho_0 = 0$ for all β , respectively, $\rho_1 = \sqrt{\frac{-\beta}{d(\beta)}} + O(\beta)$, defined for $d(0) \neq 0$ and $\beta d(\beta) < 0$, with $|\beta|$ sufficiently small. It follows from the ρ -map that $\rho_0 = 0$ is (linearly) stable if $\beta < 0$ and (linearly) unstable if $\beta > 0$. At $\beta = 0$, the stability of $\rho_0 = 0$ depends on $d(0)$, more exactly, it is (nonlinearly) stable if $d(0) < 0$, respectively, (nonlinearly) unstable if $d(0) > 0$.

When $d(0) < 0$, the second fixed point ρ_1 exists and is stable for $\beta > 0$, while if $d(0) > 0$, ρ_1 exists and is unstable for $\beta < 0$. To the fixed point ρ_1 in the ρ -map, it corresponds a closed invariant curve in the system (13).

Remark 4.2. If $d(0) \neq 0$, there exists a neighborhood of x_0 in which a unique closed invariant curve Γ_β bifurcates from x_0 as β crosses 0. More exactly, if $d(0) < 0$, the curve Γ_β exists for $\beta > 0$ and is unique and stable. It vanishes for $\beta \leq 0$. Similarly, if $d(0) > 0$, the curve Γ_β exists for any $\beta < 0$, being unique and unstable. It disappears for $\beta \geq 0$.

The Neimark-Sacker (NS) bifurcation is known also as the Andronov-Hopf bifurcation (or simply Hopf for discrete systems). We study now the NS bifurcation in the map (4). To this end, assume that the above multipliers λ^\pm are strictly complex, that is $4m - (e^{s-1} - a + 1)^2 > 0$ or $m > \frac{(m_0+4)^2}{16} \geq 0$. Consider $a \in \mathbb{R}$ as the bifurcation parameter. Then $\lambda^\pm(a) = h(a) \pm i\omega(a)$ with $h(a) = \frac{1}{2}(a - e^{s-1} + 1)$ and $\omega(a) = \frac{1}{2}\sqrt{4m - (1 + e^{s-1} - a)^2}$. In exponential form, they read

$$\lambda^\pm = r(a) e^{\pm i\theta(a)}$$

where $r(a) = \sqrt{a + m - e^{s-1}}$ and $\tan(\theta(a)) = \frac{\omega(a)}{h(a)}$, with $a + m - e^{s-1} \geq 0$. Two complex eigenvectors corresponding to the eigenvalues $\lambda^\pm(a)$ are

$$u^\pm = (\omega(a) \pm i(1 - h(a)) \quad \pm mi)^T$$

(T stands for transpose). It implies that $p = (u^+ + u^-)/2 = (\omega(a) \quad 0)^T$ and $q = (u^+ - u^-)/2i = (1 - h(a) \quad m)^T$ are two real independent vectors which lead to the transformation

$$\begin{pmatrix} x \\ y \end{pmatrix} = \begin{pmatrix} 1 - h(a) & \omega(a) \\ m & 0 \end{pmatrix} \begin{pmatrix} u \\ v \end{pmatrix}. \quad (16)$$

Using Taylor expansion of the function e^{x+s-1} at $x = 0$, the system (4) reads

$$\begin{pmatrix} \tilde{x} \\ \tilde{y} \end{pmatrix} = \begin{pmatrix} a - e^{s-1} & 1 \\ -m & 1 \end{pmatrix} \begin{pmatrix} x \\ y \end{pmatrix} + \begin{pmatrix} -\frac{x^2}{2}e^{s-1} - \frac{x^3}{6}e^{s-1} \\ 0 \end{pmatrix} + \dots$$

which, by using (16), leads to

$$\begin{pmatrix} \tilde{u} \\ \tilde{v} \end{pmatrix} = \begin{pmatrix} h(a) & -\omega(a) \\ \omega(a) & h(a) \end{pmatrix} \begin{pmatrix} u \\ v \end{pmatrix} - \begin{pmatrix} 0 \\ \frac{1}{6\omega}e^{s-1}(u + v\omega - hu)^2(u + v\omega - hu + 3) \end{pmatrix} + \dots \quad (17)$$

Finally, we can write the system (17) in complex variables $z = u + iv$, $\bar{z} = u - iv$, in the form

$$\dot{z} = r(a) e^{i\theta(a)} z + \frac{1}{2} g_{20} z^2 + g_{11} z \bar{z} + \frac{1}{2} g_{02} \bar{z}^2 + \frac{1}{2} g_{21} z^2 \bar{z} + \dots$$

where the coefficients are $g_{20} = \frac{e^{s-1} (-ih + \omega + i)^2 i}{4\omega}$, $g_{11} = -\frac{ie^{s-1} (h-1)^2 + \omega^2}{4\omega}$, $g_{02} = \frac{ie^{s-1} (ih + \omega - i)^2}{4\omega}$ and $g_{21} = \frac{e^{s-1}}{8\omega} (ih + \omega - i) (h + i\omega - 1)^2$, with $h = h(a)$ and $\omega = \omega(a)$.

The first condition leading to the NS bifurcation is $r(a) = 1$, which yields the surface

$$(NS) : a = e^{s-1} - m + 1 \stackrel{\text{not}}{=} a_{NS}.$$

On this surface, $\tan \theta_0 = \frac{\sqrt{4m-m^2}}{2-m}$, $m \in (0, 4)$, $m \neq 2$, $h_0 = \frac{1}{2}(2-m)$, $\omega_0 = \frac{1}{2}\sqrt{4m-m^2}$, $e^{i\theta_0} = \lambda^+(a_{NS}) = h_0 + i\omega_0$ with $0 < \theta_0 < \pi$. The first nondegeneracy condition $\frac{\partial r}{\partial a}(a_{NS}) = \frac{1}{2} \neq 0$ holds true independent on the parameters, while the second $e^{ik\theta_0} \neq 1$ is satisfied provided that $m \in (0, 4) \setminus \{2, 3\}$.

Expressing the coefficients g_{ij} at $a = a_{NS}$ and using (14) we obtain

$$d(0) = -\frac{e^{s-1}}{16} m (1 + e^{s-1}). \quad (18)$$

A similar result for $a(0)$ can be obtained by another method (see [11], pag. 186), namely

$$\begin{aligned} d(0) &= \frac{1}{2} \text{Re} \left\{ e^{-i\theta_0} \left[2 \left\langle p, B \left(q, (I - J)^{-1} B(q, \bar{q}) \right) \right\rangle + \left\langle p, B \left(\bar{q}, (e^{2i\theta_0} I - J)^{-1} B(q, q) \right) \right\rangle \right] \right\} \\ &\quad + \frac{1}{2} \text{Re} \left\{ e^{-i\theta_0} \langle p, C(q, q, \bar{q}) \rangle \right\} \\ &= -\frac{e^{s-1}}{16m(4-m)} (1 + e^{s-1}), \end{aligned}$$

where the vectors $p = \begin{pmatrix} m + i\sqrt{4m-m^2} \\ -2 \end{pmatrix}$ and $q = \begin{pmatrix} \frac{1}{2} \frac{i}{\sqrt{4m-m^2}} \\ -\frac{1}{4} \frac{m + i\sqrt{4m-m^2-4}}{m-4} \end{pmatrix}$ satisfy $Jq = \lambda^+ q$, $J^T p = \lambda^- p$ and $\langle p, q \rangle = 1$; B and C are given in the previous section. Since $m(4-m) > 0$, the two expressions of $d(0)$ coincide up to a positive constant. Only their sign matters in the following. Concluding, we have the following theorem.

Theorem 4.3. *If $\frac{(m_0+4)^2}{16} < m < 4$ and $m \notin \{2, 3\}$ the system (4) undergoes a NS bifurcation at a_{NS} . There exists a neighborhood of $x_0 = (0, 0)$ in which a unique closed invariant curve Γ_a bifurcates from x_0 as a crosses a_{NS} . More exactly, Γ_a is stable (by Remark 4.2) and exists for all $s \in \mathbb{R}$ and $a > a_{NS}$, with $|a - a_{NS}|$ sufficiently small.*

In Fig.2 one can see the dynamics of the map (4) for a in a neighborhood of a_{NS} , pointing out the NS bifurcation leading to a closed stable invariant curve around the origin. Notice that, if $m_0 + 4 \rightarrow 0$, m can be made sufficiently small.

The orbits on the invariant curve Γ_a can be periodic or not [11]. More exactly, if $\frac{\tilde{\varphi} - \varphi}{2\pi} = \frac{p}{q}$, with p and $q \neq 0$ integers, then any orbit of (15) starting on the closed invariant curve Γ_a is periodic, while if $\frac{\tilde{\varphi} - \varphi}{2\pi}$ is irrational, no orbit from Γ_a is periodic and all orbits on Γ_a are dense in Γ_a .

Remark 4.4. *The numerical simulations that we present in this section and in the next one are for m small, since this is the case of practical relevance.*

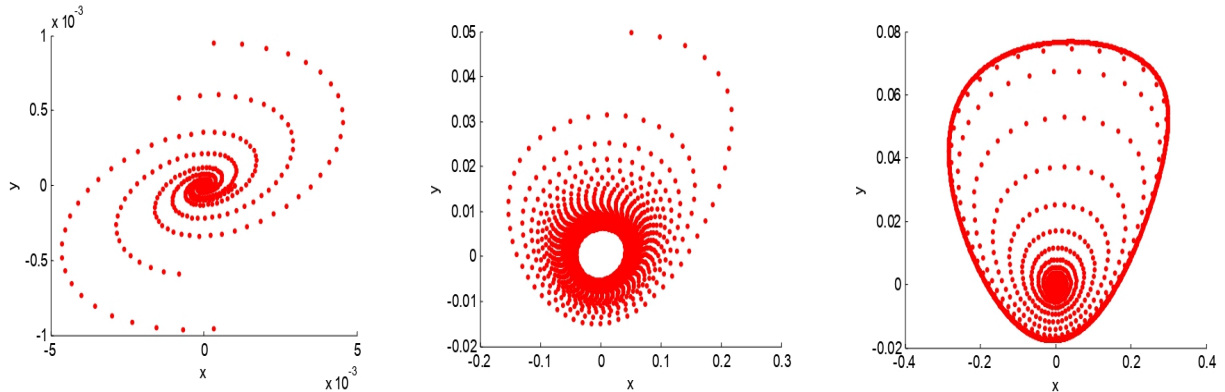


Figure 2: Dynamics of the map (4) for a in a neighborhood of a_{NS} . The parameters are $m = 0.02$, $s = 1.1$ and a) $a = 2$ (left), b) $a = a_{NS} = 2.0852$ and c) $a = 2.1$ (right). The closed stable curve exists for $a > a_{NS}$.

We illustrate in Fig.3 and Fig.4 the transition from silence to spiking regime through subthreshold oscillations. The two branches (top and bottom) in Fig.3 correspond to the highest and lowest values of the x -variable in the initial system (1), with f given by (2), for a given value of the parameter s ; the other parameters are fixed at $m = 0.02$ and $a = 2.1$. We notice that, subthreshold oscillations in Fig.3 occur when s ranges approximately in the interval $1.096 \leq s \leq 1.11$, which corresponds to $2.08 \leq a_{NS} \leq 2.09$. Thus, $a > a_{NS}$ in all these cases, which implies that subthreshold periodic orbits generated by the map (4) may arise in the behavior of the map (1).

The second nondegeneracy condition $e^{ik\theta_0} \neq 1$ leading to $m \in (0, 4) \setminus \{2, 3\}$ is important because if $e^{ik\theta_0} = 1$ for $k = 1, 2, 3, 4$, the closed curve Γ_a may not appear at all or there might be more closed invariant curves Γ_a bifurcating from $a = a_{NS}$.

5 Subthreshold oscillations in the presence of noise

Recent investigations pointed out that subthreshold activity in neurons in a noisy medium leads to the birth of spikes [2], [3], [8], [9], [14], [22]. To show this property in our model we need to apply noise to the map (1) when the parameters are in the range of subthreshold oscillations. Such ranges exist as it can be observed numerically from the bifurcation diagrams given in Fig. 3. We apply noise to the slow system in the form of a Gaussian random variable but it can be equally applied to the fast system or to both of them. The system (1) in the presence of noise added to the slow subsystem reads:

$$\begin{aligned}\tilde{x} &= f_a(x, y) \\ \tilde{y} &= y - m(x + 1 - s) + \xi,\end{aligned}\tag{19}$$

where ξ is a Gaussian random variable of zero mean value and σ standard deviation value. Fig. 5 illustrates the dynamics of the initial map (1) corresponding to subthreshold oscillations in the presence of noise. The magnitude of the noise is quantified by the standard deviation σ . In the case of m small, if the noise is small enough, say $\sigma = 0.0001$, no influence of it is observed in the dynamics of the map, Fig. 5 a). Increasing slightly 4 times the magnitude of the noise, $\sigma = 0.0004$, slow bursting of spikes are remarked, Fig. 5 b), which means

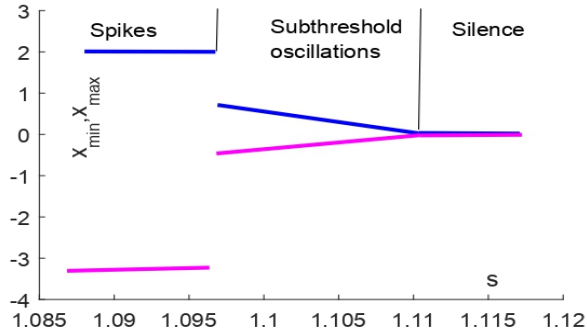


Figure 3: Transition from silence to spiking activity through subthreshold oscillations as s decreases in the system (1) for m small, $m = 0.02$, and $a = 2.1$

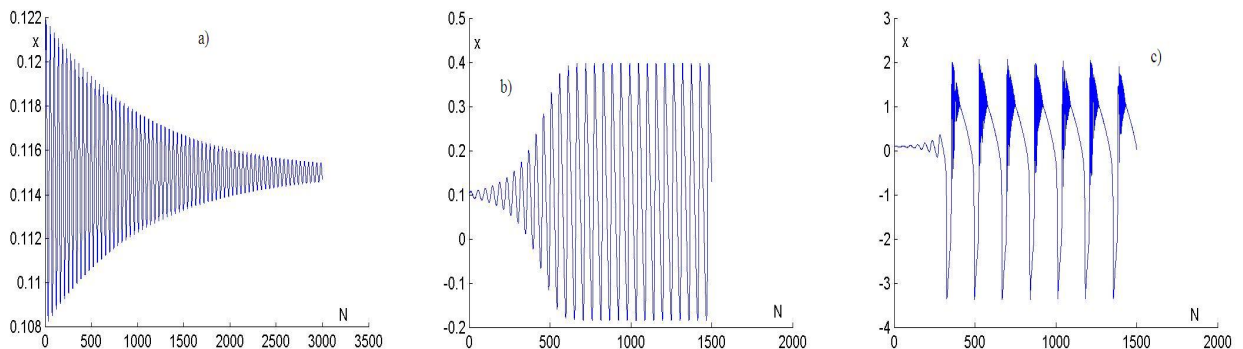


Figure 4: Transition of the dynamics of the map (1) from silence to tonic spiking through subthreshold oscillations for m small. The parameters are $a = 2.1$, $m = 0.02$ and a) $s = 1.115$, b) $s = 1.1$ and c) $s = 1.09$.

that the noise is sufficient to give a start to action potentials. A further increasing of σ , Fig. 5 c), gives rise to a tonic spiking activity.

Remark 5.1. We notice that our map produces spikes in a noisy medium not only from the regime of subthreshold oscillations but also from the regime of silence, as it can be seen from Fig. 6. Using the bifurcation diagram sketched in Fig. 3, we set the parameters at $a = 2.1$, $m = 0.02$ and $s = 1.115$ corresponding to the silence regime. While for $\sigma < 0.001$ small, Figs. 6 a)-b), no spike is observed, a slight increasing in σ , $\sigma \geq 0.002$, bursts of spikes are obtained in the map's dynamics, Fig. 6 c).

6 Conclusions

In the present work we have proposed and investigated a neuronal non-smooth map-based model to replicate individual dynamics of a neuron. This model comes as a theoretical tool in understanding subthreshold oscil-

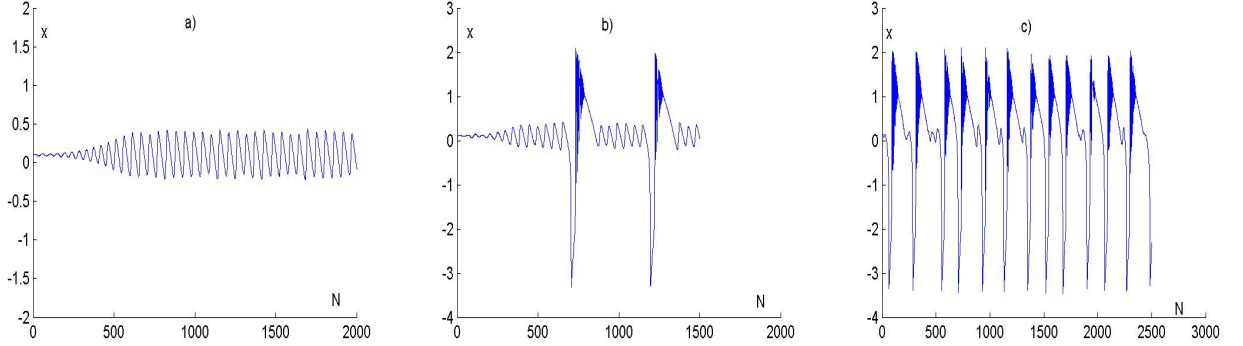


Figure 5: Noise applied to subthreshold oscillations in the map (1) for m small gives rise to spikes. The parameters are $a = 2.1$, $m = 0.02$, $s = 1.1$ and a) $\sigma = 0.0001$, b) $\sigma = 0.0004$ and c) $\sigma = 0.004$.

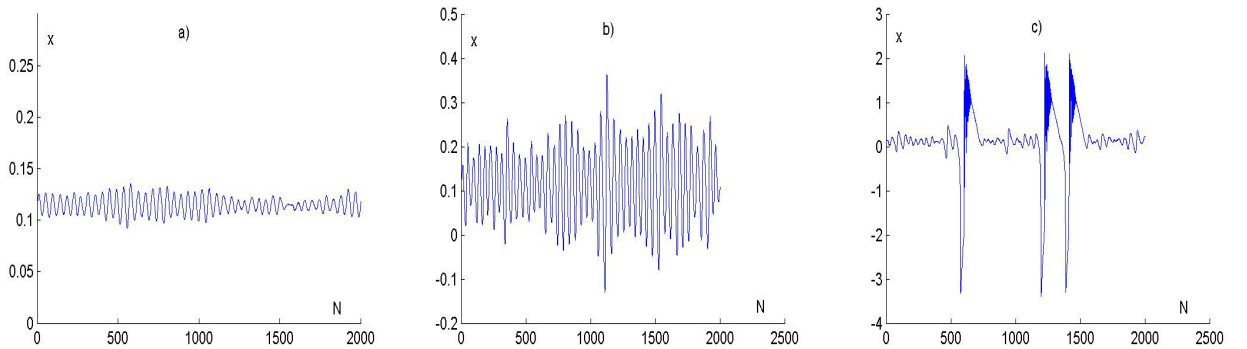


Figure 6: Noise applied to the map (1) in the silence regime for m small gives rise to spikes. The parameters are $a = 2.1$, $m = 0.02$, $s = 1.115$ and a) $\sigma = 0.0001$, b) $\sigma = 0.001$ and c) $\sigma = 0.002$.

lations in neurons. We searched for a model with a diverse dynamics in the zone of subthreshold oscillations to describe the potential behavior of a neuron. We studied the map particularly for m small ($0 < m \ll 1$) and obtained subthreshold oscillations leading and shaping spiking activity in the map. We sketched the transition from silence regime to spiking activity through subthreshold oscillations in a bifurcation diagram and illustrated its validity by numerical simulations containing waveforms of the map.

We studied then numerically if our model captures the property of action potentials of being vulnerable to noises and found that the model has this property. We applied noise to our map in the form of a Gaussian random variable and obtained bursting-spiking activity. Moreover, this property of bursts of spikes in a noisy medium is observed even though the map is in a silence regime. This is interesting and leads us to the following observation: if the noise is powerful enough a neuron is brought out from its silence suddenly, without observable delays in the subthreshold phase. This property may appear in our model due to the exponential branch of the function f_a .

7 Acknowledgments

This research was partially supported by Horizon2020-2017-RISE-777911 project.

References

- [1] I. Bashkirtseva and L. Ryashko, *Analysis of Noise-Induced Chaos-Order Transitions in Rulkov Model Near Crisis Bifurcations*, International Journal of Bifurcation and Chaos 27 (2017), pp.1–9.
- [2] I. Bashkirtseva, L. Ryashko and V. Nasyrova, *Noise-induced bursting and chaos in the two-dimensional Rulkov model*, Chaos, Solitons and Fractals 110 (2018), pp.76–81.
- [3] A. Belyaev and T. Ryazanova, *Stochastic sensitivity of attractors for a piecewise smooth neuron model*, Journal of Difference Equations and Applications 25 (2019), pp.1468–1487.
- [4] F. Buchholtz, J. Golowash, I.R. Epstain and E. Marder, *Mathematical-model of an identified stomatogastric ganglion neuron*, Journal of Neurophysiology 67 (1992), pp. 332–340.
- [5] B. Cazelles, M. Courbage and M. Rabinovich, *Anti-phase regularization of coupled chaotic maps modelling bursting neurons*, Europhysics Letters 56 (2001), pp. 504–509.
- [6] L. Cheng and H. Cao, *Synchronization Dynamics of Two Heterogeneous Chaotic Rulkov Neurons with Electrical Synapses*, International Journal of Bifurcation and Chaos 27 (2017), pp. 1–15.
- [7] D.R. Chialvo and A.V. Apkarian, *Modulated noisy biological dynamics: Three examples*, J. Stat. Physics 70 (1993), pp. 375–391.
- [8] D.T.W. Chik, Y. Wang and Z.D. Wang, *Stochastic resonance in a Hodgkin-Huxley neuron in the absence of external noise*, Physical Review E 64 (2001), pp. 1–10.
- [9] M. Heinz, K. Schafer and H.A. Braun, *Analysis of facial cold receptor activity in the rat*, Brain Research 521 (1990), pp. 289–295.
- [10] A.L. Hodgkin and A.F. Huxley, *A quantitative description of membrane current and its application to conduction and excitation in nerve*, The Journal of Physiology 117 (1952), pp. 500–544.
- [11] Y.A. Kuznetsov, *Elements of Applied Bifurcation Theory*, Springer-Verlag, 1995.
- [12] R. Llinas, *The intrinsic electrophysiological properties of mammalian neurons: insights into central nervous system function*, Science, 242(4886) (1988), pp. 1654–1664.
- [13] R. Llinas and Y. Yarom, *Electrophysiology of mammalian inferior olivary neurones in vitro. Different types of voltage-dependent ionic conductances*, J. Physiology, 315 (1981), pp. 549–567.
- [14] V. A. Makarov, V.I. Nekorkin and M.G. Velarde, *Spiking behavior in a noise-driven system combining oscillatory and excitatory properties*, Physical Review Letters, 86 (2001), pp. 1–10.
- [15] X. Meng, G. Huguet and J. Rinzel, *Type III excitability, slope sensitivity and coincidence detection*, Discrete and Continuous Dynamical Systems - Series A, 32(8) (2012), pp. 2729–2757.
- [16] N.F. Rulkov, *Modeling of spiking-bursting neural behavior using two-dimensional map*, Physical Review E, 65 (2002), 041922.

- [17] N.F. Rulkov, *Regularization of Synchronized Chaotic Bursts*, *Physical Review Letters*, 86 (2001), pp. 183–186.
- [18] A.L. Shilnikov and N.F. Rulkov, *Subthreshold oscillations in a map-based neuron model*, *Physics Letters A*, 328 (2004), pp. 177–184.
- [19] A.L. Shilnikov and N.F. Rulkov, *Origin of chaos in a two-dimensional map modeling spiking-bursting neural activity*, *IJBC* 13 (2003), pp. 3325–3340.
- [20] T. Vo, J. Tabak, R. Bertram and M. Wechselberger, *A geometric understanding of how fast activating potassium channels promote*, *J. Computational Neuroscience*, 36 (2014), pp. 259–278.
- [21] E.I. Volkov, E. Ullner, A.A. Zaikin and J. Kurths, *Oscillatory amplification of stochastic resonance in excitable systems*, *Physical Review E*, 68 (2003), pp. 1–10.
- [22] N. Zandi-Mehran, S. Panahi, Z. Hosseini, S. M. R. Hashemi Golpayegani and S. Jafari, *One dimensional map-based neuron model: A phase space interpretation*, *Chaos, Solitons and Fractals* 132 (2020), 109558.
- [23] J. Zhong, L. Zhang and G. Tigan, *Bifurcations of a discrete-time neuron model*, *Journal of Difference Equations and Applications*, 23 (2017), pp. 1508–1528.